Acta Mech Sin (2007) 23:55–63
DOI 10.1007/s10409-006-0047-0

RESEARCH PAPER

Electromagnetoelastic behaviors of functionally graded piezoelectric solid cylinder and sphere

H. L. Dai · Y. M. Fu · J. H. Yang

Received: 22 March 2006 / Revised: 12 May 2006 / Accepted: 4 July 2006 / Published online: 6 January 2007

Abstract Analytical studies on electromagnetoelastic behaviors are presented for the functionally graded piezoelectric material (FGPM) solid cylinder and sphere placed in a uniform magnetic field and subjected to the external pressure and electric loading. When the mechanical, electric and magnetic properties of the material obey an identical power law in the radial direction, the exact displacements, stresses, electric potentials and perturbations of magnetic field vector in the FGPM solid cylinder and sphere are obtained by using the infinitesimal theory of electromagnetoelasticity. Numerical examples also show the significant influence of material inhomogeneity. It is interesting to note that selecting a specific value of inhomogeneity parameter β can optimize the electromagnetoelastic responses, which will be of particular importance in modern engineering designs.

Keywords Functionally graded piezoelectric material (FGPM) · Electromagnetoelastic · Solid cylinder · Solid sphere · Perturbation of magnetic field vector

1 Introduction

The functionally graded piezoelectric material (FGPM) is a kind of piezoelectric material with material composition and properties varying continuously in certain direction. The piezoelectric devices can be entirely made of FGPM or use FGPM as a transit interlayer between two different piezoelectric materials. FGPM is the composite material intentionally designed to possess desirable properties for some specific applications. The advantage of this new kind of materials can improve the reliability or the service life of piezoelectric devices.

Recently there has been growing interest in materials with designed mechanical, electric and magnetic properties varying continuously in space on the macroscopic scale. This subject is so new that only a few results can be found in the literatures. Previous studies on the subject were performed by Wu et al. [1], Chen et al. [2] and Pan and Han [3] et al. Lim and He [4] obtained an exact solution for a compositionally graded piezoelectric layer under uniform stretch, bending and twisting. Jin and Zhong [5], Wang [6] investigated the problems of antiplane crack in the FGPM. An exact three-dimensional analysis was presented by Zhong and Shang [7] for a functionally gradient piezoelectric rectangular plate that was simply supported and grounded along its four edges. By means of an analytical-numerical method, Han and Liu [8] studied elastic waves in a functionally graded piezoelectric Cylinder. Utilizing the Fourier transform technique, Ueda [9] investigated the thermally induced fracture of a functionally graded piezoelectric layer; Sun et al. [10] investigated the behavior of a crack in the functionally graded piezoelectric/piezomagnetic materials subjected to an anti-plane shear loading. Ma et al. [11] investigated the electroelastic behavior of a Griffith crack in a functionally graded piezoelectric strip. A layerwise finite element formulation developed by Lee [12] for piezoelectric materials was used to investigated the displacement and stress response of a functionally graded piezoelectric bimorph

The project supported by China postdoctoral science foundation (20060390260) and Hunan Postdoctoral Scientific Program. The English text was polished by Yunming Chen.

H. L. Dai (✉) · Y. M. Fu · J. H. Yang
Department of Engineering Mechanics,
Hunan University, Changsha 410082, China
e-mail: hldai520@sina.com

actuator. Ootao and Tanigawa [13] studied the transient piezothermoelastic problem of a thick functionally graded thermopiezoelectric strip due to nonuniform heat supply. Guo et al. [14] investigated the transient fracture behavior of a functionally graded layered structure subjected to an in-plane impact load. Huang and Shen [15] dealt with the nonlinear vibration and dynamic response of a functionally graded material plate with surface-bonded piezoelectric layers in thermal environments. However, exact solutions for the FGPM solid cylinder and sphere in a uniform magnetic field have not been found in the literatures.

The present paper attempts to present the simple, tractable closed-form solutions for the FGPM solid cylinder and sphere. The emphasis of this research is laid on the effects of the gradient index β on the electromagnetoelastic stresses, the electric potential and the perturbation of magnetic field vector, and on the optimum design of the FGPM solid structures.

The distributions of the stresses, the electric potential and the perturbation of magnetic field vector in the FGPM solid cylinder and sphere will be calculated in this paper. a is taken as the radius of the FGPM solid cylinder and sphere. All the material constants, the magnetic permeability, the piezoelectric parameters and the dielectric parameter are assumed to have the same power-law dependence on the wall thickness of the FGPM structures, i.e.

$$\begin{aligned} c_{ij}(r) &= c_{ij}^0 r^\beta, \\ \mu(r) &= \mu_0 r^\beta, \\ e_{ri}(r) &= e_{ri}^0 r^\beta, \\ \varepsilon_{rr}(r) &= \varepsilon_{rr}^0 r^\beta, \end{aligned} \qquad (i = r,\theta;\ j = r,\theta) \tag{1}$$

where c_{ij} are the elastic constants, μ the magnetic permeability, e_{ri} the piezoelectric constants, ε_{rr} the dielectric constant, subscript 0 denotes corresponding value at the outer surfaces ($r = a$) of the FGPM solid cylinder and sphere, and β is the inhomogeneous constant determined empirically. The range $-2 \le \beta \le 2$ to be used in the present study covers all the values of coordinate exponent encountered in Refs. [7,16]. However, these β values do not necessarily represent a specific material, variable β is used to manifest the effect of inhomogeneity on the stresses, electric potential and perturbation of magnetic field vector distributions.

2 Electromagnetoelastic responses in a FGPM solid cylinder

2.1 Governing equations and solutions

A long, functionally graded piezoelectric solid cylinder with perfect conductivity is placed in a uniform magnetic field $\boldsymbol{H}(0,0,H_z)$. Let the cylindrical coordinates of a representative point be (r,θ,z). For an axisymmetry plane strain problem, the components of displacement and electric potential in the cylindrical coordinate (r,θ,z) are expressed as $u(r)$ and $\psi(r)$, and the constitutive relations are

$$\sigma_r = c_{rr}\frac{\partial u}{\partial r} + c_{r\theta}\frac{u}{r} + e_{rr}\frac{\partial \psi}{\partial r}, \tag{2a}$$

$$\sigma_\theta = c_{r\theta}\frac{\partial u}{\partial r} + c_{\theta\theta}\frac{u}{r} + e_{r\theta}\frac{\partial \psi}{\partial r}, \tag{2b}$$

$$D_r = e_{rr}\frac{\partial u}{\partial r} + e_{r\theta}\frac{u}{r} - \varepsilon_{rr}\frac{\partial \psi}{\partial r}, \tag{2c}$$

where $\sigma_i (i = r,\theta)$, D_r and ψ are the components of stresses, radial electric displacement and electric potential, respectively.

The boundary conditions are expressed as

$$\begin{aligned} &\sigma_r|_{r=a} = P_0, \\ &\psi|_{r=a} = \psi_0, \\ &u|_{r=0} = 0. \end{aligned} \tag{3}$$

Omitting the displacement electric currents, one obtains the governing electrodynamic Maxwell equations for a perfectly conducting, elastic body as [17,18]

$$\begin{aligned} &\boldsymbol{J} = \nabla \times \boldsymbol{h}, \\ &\nabla \times \boldsymbol{e} = -\mu(r)\frac{\partial \boldsymbol{h}}{\partial t}, \\ &\operatorname{div} \boldsymbol{h} = 0, \\ &\boldsymbol{e} = -\mu(r)\Big(\frac{\partial \boldsymbol{U}}{\partial t} \times \boldsymbol{H}\Big), \\ &\boldsymbol{h} = \nabla \times (\boldsymbol{U} \times \boldsymbol{H}), \end{aligned} \tag{4}$$

where $\boldsymbol{J}$ is the electric current density vector, $\boldsymbol{h}$ the perturbation of electric field vector, $\boldsymbol{e}$ the perturbation of electric field vector, $\boldsymbol{U}$ the displacement vector.

Applying an initial magnetic field vector $\boldsymbol{H}(0,0,H_z)$ in the cylindrical coordinate (r,θ,z) system to Eq. (4) yields

$$\begin{aligned} &\boldsymbol{U} = (u,0,0), \\ &\boldsymbol{e} = -\mu(r)\Big(0, H_z\frac{\partial u}{\partial t}, 0\Big), \end{aligned} \tag{5a}$$

$$\begin{aligned} &\boldsymbol{h} = (0,0,h_z), \\ &\boldsymbol{J} = \Big(0, -\frac{\partial h_z}{\partial r}, 0\Big), \\ &h_z = -H_z\Big(\frac{\partial u}{\partial r} + \frac{u}{r}\Big). \end{aligned} \tag{5b}$$

The equilibrium equation of the FGPM solid cylinder, in the absence of body forces, is expressed as

$$\frac{\partial \sigma_r}{\partial r} + \frac{\sigma_r - \sigma_\theta}{r} + f_z = 0, \tag{6}$$

where f_z is defined as Lorentz's force which may be written as [17,18]

$$f_z = \mu_0 H_z^2 \frac{\partial}{\partial r}\left(r^\beta \frac{\partial u}{\partial r} + r^\beta \frac{u}{r}\right). \tag{7}$$

In the absence of free charge density, the charge equation of electrostatics is expressed as [19]

$$\frac{\partial D_r}{\partial r} + \frac{D_r}{r} = 0, \quad (0 \le r \le a). \tag{8}$$

Solving Eq. (8), one gets $D_r = 0$

Thus, Eq. (2c) may be rewritten as

$$\frac{\partial \psi}{\partial r} = \frac{e_{rr}}{\varepsilon_{rr}} \frac{\partial u}{\partial r} + \frac{e_{r\theta}}{\varepsilon_{rr}} \frac{u}{r}. \tag{9}$$

Substituting Eq. (9) into Eqs. (2a), (2b) and utilizing Eq. (1) yields

$$\sigma_r = C_1 r^\beta \frac{\partial u}{\partial r} + C_2 r^\beta \frac{u}{r}, \tag{10a}$$

$$\sigma_\theta = C_2 r^\beta \frac{\partial u}{\partial r} + C_3 r^\beta \frac{u}{r}, \tag{10b}$$

where

$$\begin{aligned} C_1 &= c_{rr}^0 + \frac{e_{rr}^0 e_{rr}^0}{\varepsilon_{rr}^0}, \\ C_2 &= c_{r\theta}^0 + \frac{e_{rr}^0 e_{r\theta}^0}{\varepsilon_{rr}^0}, \\ C_3 &= c_{\theta\theta}^0 + \frac{e_{r\theta}^0 e_{r\theta}^0}{\varepsilon_{rr}^0}. \end{aligned} \tag{11}$$

By substituting Eqs. (10), (7) into Eq. (6), the equilibrium equation is expressed as

$$\frac{\partial^2 \mathrm{u}}{\partial r^2} + (\beta + 1)\frac{1}{r}\frac{\partial u}{\partial r} + \Delta \frac{u}{r^2} = 0, \tag{12}$$

where $\Delta = \dfrac{C_2\beta - C_3 + \mu_0 H_z^2(\beta - 1)}{C_1 + \mu_0 H_z^2}$.

It is obvious that the homogeneous solution to Eq. (12) can be obtained by assuming

$$u = K r^m, \tag{13}$$

where K is an arbitrary constant, substituting Eq. (13) into Eq. (12), one obtains

$$m^2 + \beta m + \Delta = 0, \tag{14}$$

Thus, the characteristic equation's roots are

$$\begin{aligned} m_1 &= \frac{1}{2}\left(-\beta + \sqrt{\beta^2 - 4\Delta}\right), \\ m_2 &= \frac{1}{2}\left(-\beta - \sqrt{\beta^2 - 4\Delta}\right). \end{aligned} \tag{15}$$

These roots may be (a) real, distinct, (b) double roots, (c) complex conjugate. For real distinct roots, the solution is

$$u = A_1 r^{m_1} + A_2 r^{m_2}, \tag{16}$$

where A_1 and A_2 are unknown constants.

For double roots $m_1 = m_2 = m$, the solution becomes

$$u = (A_1 + A_2 \ln r) r^m. \tag{17}$$

In the case of complex roots $m_1 = x + y\mathrm{i}$, $m_2 = x - y\mathrm{i}$, the solution takes the form

$$u = [A_1 \cos(y \ln r) + A_2 \sin(y \ln r)] r^x. \tag{18}$$

For the numerical values to be used ($\Delta < 0$ and $-2 \le \beta \le 2$), only real, distinct roots will be obtained. Thus, the stress expressions will be obtained by using Eq. (16)

$$\begin{aligned} \sigma_r = {} & (C_1 m_1 + C_2) A_1 r^{m_1 + \beta - 1} \\ & + (C_1 m_2 + C_2) A_2 r^{m_2 + \beta - 1}, \end{aligned} \tag{19a}$$

$$\begin{aligned} \sigma_\theta = {} & (C_2 m_1 + C_3) A_1 r^{m_1 + \beta - 1} \\ & + (C_2 m_2 + C_3) A_2 r^{m_2 + \beta - 1}. \end{aligned} \tag{19b}$$

By integrating Eq. (9) and utilizing Eq. (16), one have

$$\psi = \frac{e_{rr} m_1 + e_{r\theta}}{\varepsilon_{rr} m_1} A_1 r^{m_1} + \frac{e_{rr} m_2 + e_{r\theta}}{\varepsilon_{rr} m_2} A_2 r^{m_2}. \tag{20}$$

From Eq. (3), Eq. (19a) and Eq. (20), one gets

$$\begin{aligned} A_1 &= \frac{k_4 P_0 - k_2 \psi_0}{k_1 k_4 - k_2 k_3}, \\ A_2 &= \frac{k_3 P_0 - k_1 \psi_0}{k_2 k_3 - k_1 k_4}, \end{aligned} \tag{21}$$

where

$$\begin{aligned} k_1 &= (C_1 m_1 + C_2) a^{m_1 + \beta - 1}, \\ k_2 &= (C_1 m_2 + C_2) a^{m_2 + \beta - 1}, \\ k_3 &= \frac{e_{rr} m_1 + e_{r\theta}}{\varepsilon_{rr} m_1} a^{m_1}, \\ k_4 &= \frac{e_{rr} m_2 + e_{r\theta}}{\varepsilon_{rr} m_2} a^{m_2}. \end{aligned} \tag{22}$$

Thus, the exact stresses, electric potential and perturbation of magnetic field vector are obtained as follows:

$$\sigma_r = [(C_1 m_1 + C_2)(k_4 P_0 - k_2 \psi_0) r^{m_1+\beta-1} + (C_1 m_2 + C_2)(k_1 \psi_0 - k_3 P_0) r^{m_2+\beta-1}]/(k_1 k_4 - k_2 k_3), \tag{23a}$$

$$\sigma_r = [(C_2 m_1 + C_3)(k_4 P_0 - k_2 \psi_0) r^{m_1+\beta-1} + (C_2 m_2 + C_3)(k_1 \psi_0 - k_3 P_0) r^{m_2+\beta-1}]/(k_1 k_4 - k_2 k_3), \tag{23b}$$

$$\psi = \frac{e_{rr} m_1 + e_{r\theta}}{\varepsilon_{rr} m_1} \frac{k_4 P_0 - k_2 \psi_0}{k_1 k_4 - k_2 k_3} r^{m_1} + \frac{e_{rr} m_2 + e_{r\theta}}{\varepsilon_{rr} m_2} \frac{k_3 P_0 - k_1 \psi_0}{k_2 k_3 - k_1 k_4} r^{m_2}, \tag{23c}$$

$$h_z = -H_z \Big[(m_1 + 1) \frac{k_4 P_0 - k_2 \psi_0}{k_1 k_4 - k_2 k_3} r^{m_1-1} + (m_2 + 1) \frac{k_3 P_0 - k_1 \psi_0}{k_2 k_3 - k_1 k_4} r^{m_2-1} \Big]. \tag{23d}$$

2.2 Numerical results and discussion

The electromagnetoelastic responses are considered for an FGPM solid cylinder placed in a uniform magnetic field and subjected to the external pressure and electric loading. In the numerical calculations, the following material constants for the FGPM solid cylinder are adopted [20,21]:

$c_{rr}^0 = 110.0\,\text{GPa}$, $c_{r\theta}^0 = 77.8\,\text{GPa}$,
$c_{rz}^0 = c_{\theta z}^0 = 115.0\,\text{GPa}$, $c_{\theta\theta}^0 = 220.0\,\text{GPa}$,
$e_{rr}^0 = 15.1\,\text{C/m}^2$, $e_{r\theta}^0 = -5.2\,\text{C/m}^2$,
$\varepsilon_{rr}^0 = 5.62 \times 10^{-9}\,\text{C}^2/\text{Nm}^2$, $\mu_0 = 4\pi \times 10^{-7}\,\text{H/m}$,
$H_z = 1.796 \times 10^9\,\text{A/m}$.

The radius of the FGPM solid cylinder is taken as $a = 0.01\,\text{m}$. The center point is taken as $r = 1 \times 10^{-6}\,\text{m}$ in the calculation to ensure the precision of the result. In all the examples, the gradient index β of the material properties takes five values: -1.5, -1, 0, 1, 1.5.

Example 1 The corresponding boundary conditions are expressed as

$$\sigma_r|_{r=a} = -p_0, \quad \psi|_{r=a} = 0, \tag{24}$$

where p_0 expresses the constant pressure, and dimensionless variables $R = r/a$, $\sigma_i^* = \sigma_i/p_0 (i = r, \theta)$ and $h_z^* = h_z/H_z$ are adopted in the calculations.

The radial stress, circumferential stress and electric potential distributions in the FGPM solid cylinder are shown in Figs. 1, 2 and 3, respectively. The radial stresses

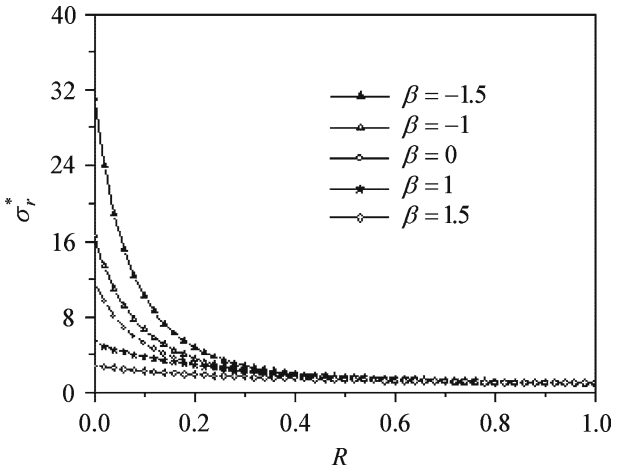

Fig. 1 Radial stress distribution for FGPM solid cylinder subjected to external pressure

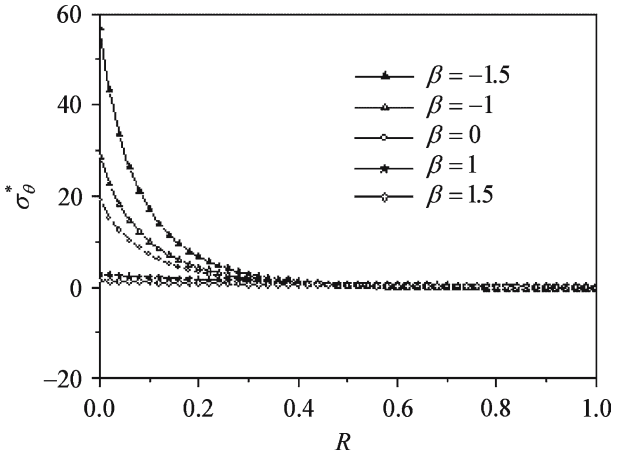

Fig. 2 Circumferential stress distribution for FGPM solid cylinder subjected to external pressure

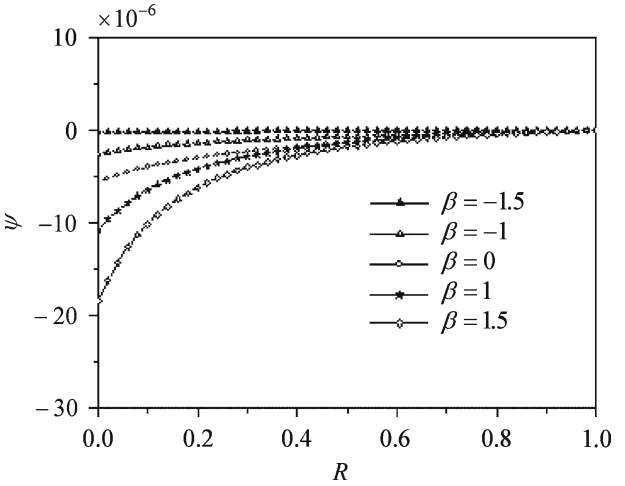

Fig. 3 Electric potential distribution for FGPM solid cylinder subjected to external pressure

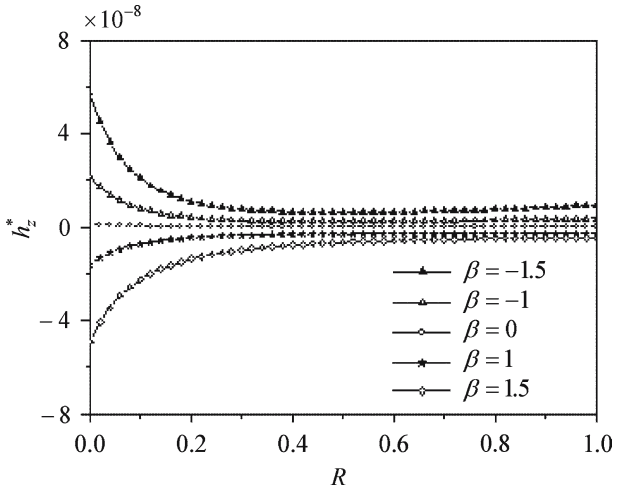

Fig. 4 The perturbation of magnetic field vector distribution for FGPM solid cylinder subjected to external pressure

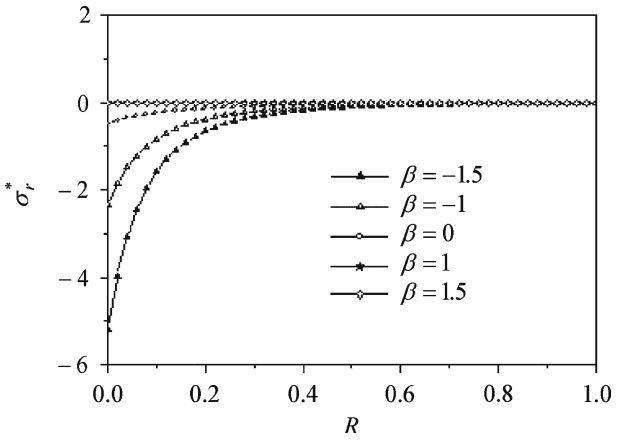

Fig. 5 Radial stress distribution for FGPM solid cylinder subjected to external electric potential

corresponding to different β at $R = 1$ are equal to 1, which satisfies the external boundary condition (24) (see Fig. 1). The values of stresses are increasing as the position is approaching the center of the FGPM solid cylinder; and the increasing trend of the curve becomes milder with increasing β (see Figs. 1, 2). The distribution of electric potential are just opposite to that of the stresses (see Fig. 3). Then, its values are very small in the case of FGPM solid cylinder subjected to external pressure. The variation of perturbation of magnetic field vector in Fig. 4 is different from that shown in Figs. 1, 2 and 3, and the trend is affected greatly by the β value.

Example 2 The corresponding boundary conditions are expressed as

$$\sigma_r|_{r=a} = 0, \quad \psi|_{r=a} = \psi_0, \tag{25}$$

where ψ_0 expresses the constant electric potential, and $\sigma_i^* = \sigma_i/c_{rr}^0 (i = r, \theta)$, $\psi^* = \psi/\psi_0$ and $h_z^* = h_z/H_z$ are adopted in the calculations.

The radial stress and electric potential distributions in the FGPM solid cylinder subjected to external electric loading are shown in Figs. 5 and 6. The radial stresses and the electric potential corresponding to different β at $R = 1$ are, respectively, equal to 0 and 1, which satisfy the external boundary condition (25). The absolute values of stresses is increasing gradually as the position is approaching the center of the FGPM solid cylinder; and the increasing trend of the curve becomes milder with increasing β. The distribution of perturbation of magnetic field vector is shown in Fig. 7. The values of perturbation of magnetic field vector in the case of FGPM solid cylinder subjected to the electric loading are bigger than those in the case of FGPM solid cylinder subjected to external pressure.

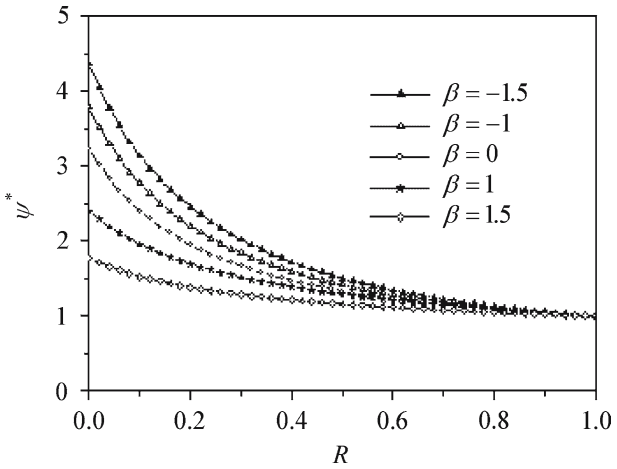

Fig. 6 Electric potential distribution for FGPM solid cylinder subjected to external electric potential

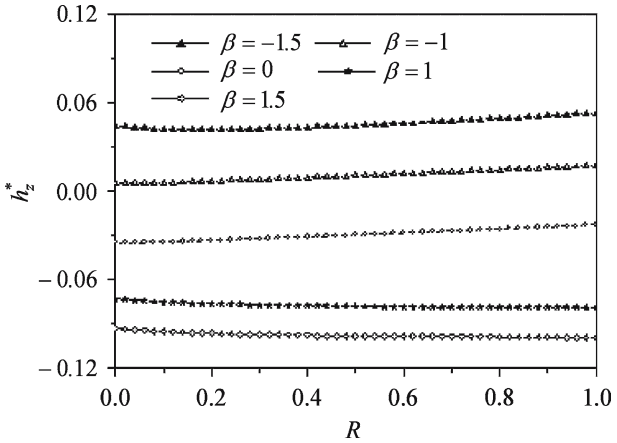

Fig. 7 The perturbation of magnetic field vector distribution for FGPM solid cylinder subjected to external electric potential

3 Electromagnetoelastic responses in an FGPM solid sphere

3.1 Basic formulations and solutions

An FGPM solid sphere with perfect conductivity is placed in a uniform magnetic field $\boldsymbol{H}(0,0,H_\phi)$. Let the spherical coordinates of any representative point be (r,θ,ϕ), the components of displacement and electric potential in the spherical coordinate (r,θ,ϕ) are expressed as $u(r)$ and $\psi(r)$, the constitutive relations are [22,23]

$$\sigma_r = c_{rr}\frac{\partial u}{\partial r} + 2c_{r\theta}\frac{u}{r} + e_{rr}\frac{\partial \psi}{\partial r}, \tag{26a}$$

$$\sigma_\theta = c_{r\theta}\frac{\partial u}{\partial r} + (c_{\theta\theta}+c_{\theta\phi})\frac{u}{r} + e_{r\theta}\frac{\partial \psi}{\partial r}, \tag{26b}$$

$$D_r = e_{rr}\frac{\partial u}{\partial r} + 2e_{r\theta}\frac{u}{r} - \varepsilon_{rr}\frac{\partial \psi}{\partial r}. \tag{26c}$$

Omitting the displacement electric currents, one obtains the governing electrodynamic Maxwell equations for a perfectly conducting, elastic body as

$$\begin{aligned}
&\boldsymbol{J} = \nabla \times \boldsymbol{h},\\
&\nabla \times \boldsymbol{e} = -\mu(r)\frac{\partial \boldsymbol{h}}{\partial t},\\
&\mathrm{div}\boldsymbol{h} = 0,\\
&\boldsymbol{e} = -\mu(r)\Big(\frac{\partial \boldsymbol{U}}{\partial t} \times \boldsymbol{H}\Big),\\
&\boldsymbol{h} = \nabla \times (\boldsymbol{U} \times \boldsymbol{H}).
\end{aligned} \tag{27}$$

Applying an initial magnetic field vector $\boldsymbol{H}(0,0,H_\phi)$ in the spherical coordinate (r,θ,ϕ) system to Eq. (27) yields [18,24]

$$\begin{aligned}
&\boldsymbol{U} = (u,0,0),\\
&\boldsymbol{e} = -\mu(r)\Big(0, H_\phi\frac{\partial u}{\partial t}, 0\Big),
\end{aligned} \tag{28a}$$

$$\begin{aligned}
&\boldsymbol{h} = (0,0,h_\phi),\\
&\boldsymbol{J} = \Big(0, -\frac{\partial h_\phi}{\partial r}, 0\Big),\\
&h_\phi = -H_\phi\Big(\frac{\partial u}{\partial r} + \frac{2u}{r}\Big).
\end{aligned} \tag{28b}$$

The electomagnetic dynamic equation of the FGPM solid sphere, in the absence of body forces, is expressed as

$$\frac{\partial \sigma_r}{\partial r} + \frac{2(\sigma_r - \sigma_\theta)}{r} + f_\phi = 0, \tag{29}$$

where f_ϕ is defined as Lorentz's force [17] which may be written as

$$f_\phi = \mu_0 H_\phi^2 \frac{\partial}{\partial r}\Big(r^\beta \frac{\partial u}{\partial r} + r^\beta \frac{2u}{r}\Big). \tag{30}$$

In the absence of free charge density, the charge equation of electrostatics [19] is expressed as

$$\frac{\partial D_r}{\partial r} + \frac{2D_r}{r} = 0, \quad (0 \le r \le a). \tag{31}$$

Solving Eq. (31) gives $D_r = 0$.

Thus, Eq. (26c) may be rewritten as

$$\frac{\partial \psi}{\partial r} = \frac{e_{rr}}{\varepsilon_{rr}}\frac{\partial u}{\partial r} + 2\frac{e_{r\theta}}{\varepsilon_{rr}}\frac{u}{r}. \tag{32}$$

Substituting Eq. (32) into Eqs. (26a), (26b) and utilizing Eq. (1), one obtains

$$\sigma_r = C_1 r^\beta \frac{\partial u}{\partial r} + 2C_2 r^\beta \frac{u}{r}, \tag{33a}$$

$$\sigma_\theta = C_2 r^\beta \frac{\partial u}{\partial r} + C_4 r^\beta \frac{u}{r}, \tag{33b}$$

where $C_4 = c^0_{\theta\theta} + c^0_{\theta\phi} + 2\dfrac{e^0_{r\theta}e^0_{r\theta}}{\varepsilon^0_{rr}}$, and C_i $(i = 1,2,3)$ is the same as Eq. (11).

Substituting Eqs. (33) and Eq. (30) into Eq. (29) yields

$$\frac{\partial^2 u}{\partial r^2} + (\beta+2)\frac{1}{r}\frac{\partial u}{\partial r} + \lambda\frac{u}{r^2} = 0, \tag{34}$$

where $\lambda = \dfrac{2[C_2(\beta+1) - C_4 + \mu_0 H_\phi^2(\beta-1)]}{C_1 + \mu_0 H_\phi^2}$.

The solution of Eq. 34 gives

$$\begin{aligned}
\sigma_r = {} & [(C_1 s_1 + 2C_2)(l_4 P_0 - l_2\psi_0) r^{s_1+\beta-1}\\
& + (C_1 s_2 + 2C_2)(l_1\psi_0 - l_3 P_0) r^{s_2+\beta-1}]/(l_1 l_4 - l_2 l_3),
\end{aligned} \tag{35a}$$

$$\begin{aligned}
\sigma_r = {} & [(C_2 s_1 + C_4)(l_4 P_0 - l_2\psi_0) r^{s_1+\beta-1}\\
& + (C_2 s_2 + C_4)(l_1\psi_0 - l_3 P_0) r^{s_2+\beta-1}]/(l_1 l_4 - l_2 l_3),
\end{aligned} \tag{35b}$$

$$\begin{aligned}
\psi = {} & \frac{e_{rr}s_1 + 2e_{r\theta}}{\varepsilon_{rr}s_1}\frac{l_4 P_0 - l_2\psi_0}{l_1 l_4 - l_2 l_3} r^{s_1}\\
& + \frac{e_{rr}s_2 + 2e_{r\theta}}{\varepsilon_{rr}s_2}\frac{l_3 P_0 - l_1\psi_0}{l_2 l_3 - l_1 l_4} r^{s_2},
\end{aligned} \tag{35c}$$

$$\begin{aligned}
h_\phi = {} & -H_\phi\Big[(s_1+2)\frac{l_4 P_0 - l_2\psi_0}{l_1 l_4 - l_2 l_3} r^{s_1-1}\\
& + (s_2+2)\frac{l_3 P_0 - l_1\psi_0}{l_2 l_3 - l_1 l_4} r^{s_2-1}\Big].
\end{aligned} \tag{35d}$$

The detailed solving process for Eq. (34) is given in Appendix A.

3.2 Numerical results and discussion

The electromagnetoelastic responses are studied for an FGPM solid sphere placed in a uniform magnetic field and subjected to the external pressure and the electric loading.

Example 3 All conditions are the same as those for example 1. The electromagneto elastic stresses and the electric potential distributions in the FGPM solid sphere subjected to the external pressure are shown in Figs. 8 and 9, respectively. The stresses and electric potential distributions have the same trend as those in Figs. 1 and 3, but the magnitude in the case of FGPM solid sphere are larger than that in the case of FGPM solid cylinder. The same trend in the perturbation of magnetic field vector of the FGPM cylindrical vessels is observed by comparing Figs. 4 with 10; however, the magnitudes in the case of FGPM solid sphere are smaller than those in the case of FGPM solid cylinder. The curves have the same trend even though the structure is different.

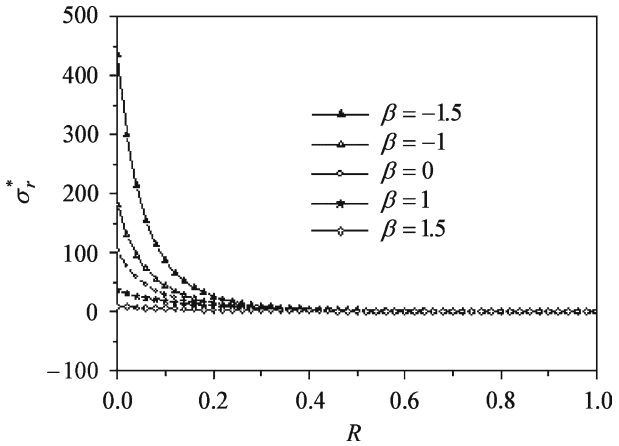

Fig. 8 Radial stress distribution for FGPM solid sphere subjected to external pressure

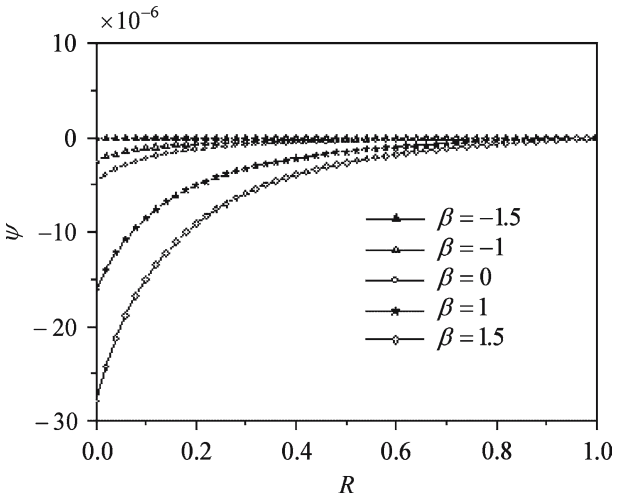

Fig. 9 Electric potential distribution for FGPM solid sphere subjected to external pressure

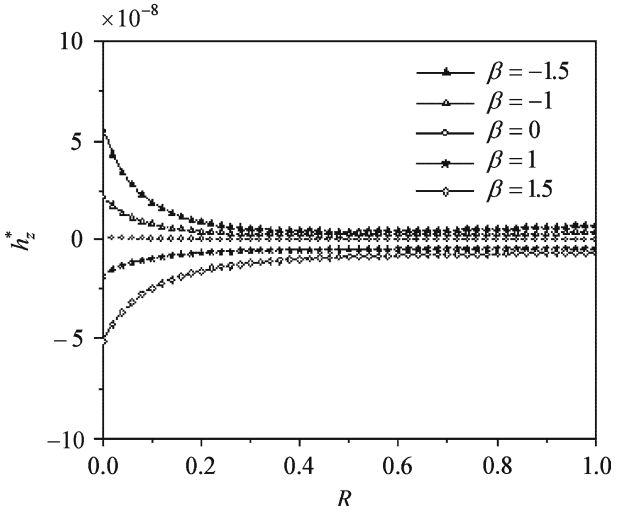

Fig. 10 The perturbation of magnetic field vector distribution for FGPM solid sphere subjected to external pressure

4 Conclusions

1. Exact solutions are obtained by means of the infinitesimal theory of electromagnetoelasticity for the FGPM solid structures in a uniform magnetic field and subjected to the external pressure and electric loading. The mechanical, electric and magnetic properties of the material are assumed to have the same exponent-law dependence in the radial direction of the FGPM solid structures. The solution is valid for arbitrary mechanical and electric loads exerted on the external surface of the FGPM solid structures.
2. The pure electric loading case has several characteristics different from those of the pure mechanical loading cases. Thus, applying proper mechanical and electric loads to the FGPM solid structures can control the distributions of stresses, electric potential and perturbation of magnetic field vector in the FGPM solid structures.
3. The gradient index β has a great effect on the stresses, electric potential and perturbation of magnetic field vector of the FGPM solid structures. Thus selecting a proper β value, engineers can design a specific FGPM solid structure that can meet some special requirements.

4. Although this paper considers the material constants of only power function in the radial direction, its technique is applicable to other inhomogeneous material.

Appendix A

The solution of Eq. (34) for homogeneous materials can be obtained by assuming

$$u = Kr^s. \tag{A1}$$

where K is an arbitrary constant. Substituting Eq. (A1) into Eq. (34), one obtains

$$s^2 + (\beta + 1)s + \lambda = 0, \tag{A2}$$

Thus, the characteristic equation's roots are

$$\begin{aligned} s_1 &= \frac{1}{2}\big(-\beta - 1 + \sqrt{(\beta-1)^2 - 4\lambda}\big), \\ s_2 &= \frac{1}{2}\big(-\beta - 1 - \sqrt{(\beta-1)^2 - 4\lambda}\big). \end{aligned} \tag{A3}$$

Here also, only real, distinct roots will be considered ($\lambda < 0$ and $-2 \le \beta \le 2$). The general solution to Eq. (34) is

$$u = B_1 r^{s_1} + B_2 r^{s_2}, \tag{A4}$$

where B_1 and B_2 are unknown constants. By virtue of Eq. (A4), the expressions of the radial and circumferential stresses for the FGPM solid sphere are derived as follows:

$$\begin{aligned} \sigma_r = {} & (C_1 s_1 + 2C_2) B_1 r^{s_1+\beta-1} \\ & + (C_1 s_2 + 2C_2) B_2 r^{s_2+\beta-1}, \end{aligned} \tag{A5a}$$

$$\begin{aligned} \sigma_\theta = {} & (C_2 s_1 + C_4) B_1 r^{s_1+\beta-1} \\ & + (C_2 s_2 + C_4) B_2 r^{s_2+\beta-1}. \end{aligned} \tag{A5b}$$

Integrating Eq. (27) and utilizing Eq. (A4), one has

$$\psi = \frac{e_{rr}s_1 + 2e_{r\theta}}{\varepsilon_{rr}s_1} B_1 r^{s_1} + \frac{e_{rr}s_2 + 2e_{r\theta}}{\varepsilon_{rr}s_2} B_2 r^{s_2}. \tag{A6}$$

By means of the boundary condition (3), Eq. (A5a) and Eq. (A6), one gets

$$\begin{aligned} B_1 &= \frac{l_4 P_0 - l_2 \psi_0}{l_1 l_4 - l_2 l_3}, \\ B_2 &= \frac{l_3 P_0 - l_1 \psi_0}{l_2 l_3 - l_1 l_4}, \end{aligned} \tag{A7}$$

where

$$\begin{aligned} l_1 &= (C_1 s_1 + 2C_2) a^{s_1+\beta-1}, \\ l_2 &= (C_1 s_2 + 2C_2) a^{s_2+\beta-1}, \\ l_3 &= \Big(\frac{e_{rr}}{\varepsilon_{rr}} s_1 + 2\frac{e_{r\theta}}{\varepsilon_{rr}}\Big)\frac{a^{s_1}}{s_1}, \\ l_4 &= \Big(\frac{e_{rr}}{\varepsilon_{rr}} s_2 + 2\frac{e_{r\theta}}{\varepsilon_{rr}}\Big)\frac{a^{s_2}}{s_2}. \end{aligned} \tag{A8}$$

Thus, the Eqs. (35) can be easily obtained by substituting Eq. (A7) into Eqs. (A5), Eq. (A6) and the last term of Eq. (28).

References

1. Wu, C.C.M., Kahn, M., Moy, W.: Piezoelectric ceramics with functional gradients: a new application in material design. J. Am. Ceramics Soc. **79**, 809–812 (1996)
2. Chen, J., Liu, Z., Zou, Z.: Dynamic response of a crack in a functionally graded interface of two dissimilar piezoelectric half-planes. Arc. Appl. Mech. **72**, 686–696 (2003)
3. Pan, E., Han, F.: Exact solution for functionally graded and layered magneto-electro-elastic plates. Int. J. Eng. Sci. **43**, 321–339 (2005)
4. Lim, C.W., He, L.H.: Exact solution of a compositionally graded piezoelectric layer under uniform stretch, bending and twisting. Int. J. Mech. Sci. **43**, 2479–2492 (2001)
5. Jin, B., Zhong, Z.: A moving mode-III crack in functionally graded piezoelectric material: permeable problem. Mech. Res. Commun. **29**, 217–224 (2002)
6. Wang, B.L.: A mode-III crack in functionally graded piezoelectric materials. Mech. Res. Commun. **30**, 151–159 (2003)
7. Zhong, Z., Shang, E.T.: Three-dimensional exact analysis of a simply supported functionally gradient piezoelectric plate. Int. J. Solids Struct. **40**, 5335–5352 (2003)
8. Han, X., Liu, G.R.: Elastic waves in a functionally graded piezoelectric cylinder. Smart Materials Struct. **12**, 962–971 (2003)
9. Ueda, S.: Thermally induced fracture of a functionally graded piezoelectric layer. Journal of Thermal Stresses, **27**, 291–309 (2004)
10. Sun, J.L., Zhou, Z.G., Wang, B.: A permeable crack in functionally graded piezoelectric/piezomagnetic materials (in Chinese). Acta Mech. Sin. **37**(1), 9–14 (2005)
11. Ma, L., Wu, L.Z., Zhou, Z.G. et al.: Fracture analysis of a functionally graded piezoelectric strip. Composite Struct. **69**, 294–300 (2005)
12. Lee, H.J.: Layerwise laminate analysis of functionally graded piezoelectric bimorph beams. J. Intell. Material Syst. Struct. **16**, 365–371 (2005)
13. Ootao, Y., Tanigawa, Y.: The transient piezothermoelastic problem of a thick functionally graded thermopiezoelectric strip due to nonuniform heat supply. Arch. Appl. Mech. **74**, 449–465 (2005)
14. Guo, L.C., Wu, L.Z., Sun, Y.G. et al.: The transient fracture behavior for a functionally graded layered structure subjected to an in-plane impact load. Acta Mech. Sin. **21**, 257–266 (2005)
15. Huang, X.L., Shen, H.S.: Vibration and dynamic response of functionally graded plates with piezoelectric actuators in thermal environments. J. Sound Vibr. **289**, 25–53 (2006)

16. Tarn, J.Q.: Exact solutions for functionally graded anisotropic cylinders subjected to thermal and mechanical loads. Int. J. Solids Struct. **38**, 8189–8206 (2001)
17. John, K.D.: Electromagnetic. McGraw-Hill, Inc., USA (1984)
18. Dai, H.L., Wang, X.: Dynamic responses of piezoelectric hollow cylinders in an axial magnetic field. Int. J. Solids Struct. **41**, 5231–5246 (2004)
19. Heyliger, P.: A note on the static behavior of simply-supported laminated piezoelectric cylinders. Int. J. Solids Struct. **34**, 3781–3794 (1996)
20. Dunn, M.L., Taya, M.: Electroelastic field concentrations in and around inhomogeneities in piezoelectric solids. J. Appl. Mech. **61**, 474–475 (1994)
21. Dai, H.L., Wang, X.: Transient wave propagation in piezoelectric hollow spheres subjected to thermal shock and electric excitation. Struct Eng. Mech. **19**(4), 441–457 (2005)
22. Sinha, D.K.: Note on the radial deformation of a piezoelectric polarized spherical shell with symmetrical temperature distribution. J. Acoust. Soc. Am. **34**, 1073–1075 (1962)
23. Dai, H.L., Wang, X.: Thermo-electro-elastic transient responses in piezoelectric hollow structures. Int. J. Solids Struct. **42**, 1151–1171 (2005)
24. William, H.: Engineering Electromagnetics, 6th edn. McGraw-Hill, Inc., USA (2002)